

All solid state laser source for tunable blue and ultraviolet radiation

C. Zimmermann, V. Vuletic, A. Hemmerich, and T. W. Hänsch
Sektion Physik der Universität München, 80799, München, Germany

(Received 22 November 1994; accepted for publication 16 February 1995)

Tunable blue and ultraviolet single mode laser light has been generated by frequency quadrupling the output of a semiconductor laser with two successive frequency doubling stages. The laser source is based on a commercial high power semiconductor laser near 972 nm which combines a low power single mode master oscillator with a high power amplifier. The doubling stages consist of nonlinear crystals which are placed inside compact optical buildup resonators. Up to 156 mW tunable blue radiation near 486 nm and 2.1 mW ultraviolet light near 243 nm have been produced. © 1995 American Institute of Physics.

Modern semiconductor lasers are almost ideal light sources for a large number of applications. They are efficient, reliable, and compact. The use of laser diodes is limited only by their wavelength range which is typically restricted to the red and infrared part of the spectrum. However, a compact blue or ultraviolet laser source would have interesting technological applications for thermal printing, lithography, laser television, satellite communication, optical data storage, and spectroscopic analysis.^{1,2} A number of research groups are currently concentrating on expanding the range of semiconductor laser radiation to shorter wavelengths. The different approaches range from developing laser diodes which emit directly in the blue^{3,4} to various techniques for frequency conversion of infrared radiation.⁵⁻⁷

Our work on this subject is originally motivated by the interest in a highly monochromatic laser source for spectroscopy of the hydrogen $1s-2s$ transition near 243 nm.⁸ Precision measurements based on this transition have recently yielded an accurate value for the Rydberg constant,⁹ and have provided a stringent test of the quantum electrodynamic theory for a bound system.¹⁰ In these experiments, ultraviolet laser radiation has been generated with a complex laser system based on a frequency doubled single mode dye ring laser near 486 nm.¹¹ As the only one available to date, this method is expensive and lacks the reliability which is desirable for further experiments.

In this letter we present a compact and inexpensive alternative. Ultraviolet light is generated by frequency quadrupling the output of a high power semiconductor laser with two frequency doubling stages. The source is easily transportable and new spectroscopic experiments with trapped hydrogen or even antihydrogen are conceivable. Such experiments demand a sophisticated and highly specialized atomic preparation technique which is available only at very few laboratories in the world.¹² As another scientific application, the laser source would allow for the construction of a reasonably sized optical hydrogen frequency standard.

The laser source (Fig. 1) is based on a commercially available semiconductor "master oscillator power amplifier" (MOPA) (SDL-5760),¹³ which is a combination of a strained quantum well distributed Bragg reflector laser followed by a single pass semiconductor power amplifier. The resonator of the master laser is formed by two micro-fabricated gratings which guarantee stable single mode

operation.¹⁴ The laser wavelength may be tuned with temperature at a rate of 0.07 nm/K. A rapid frequency scan is possible by varying the injection current (0.35 GHz/mA). The master oscillator is followed by a flared amplifier. The MOPA is originally delivered in a sealed housing including a Peltier cooler and some beam shaping optics. At room temperature the laser provides 1 W radiation at 970.3 nm. The operating current is specified by the manufacturer to be 250 mA for the master oscillator and 3.5 A for the power amplifier.

By observing the frequency spectrum with an optical Fabry-Pérot spectrum analyzer we found that reliable tunable single mode operation could not be achieved because of uncontrolled optical feedback from the beam shaping optics. To get control over the optical elements we have removed the MOPA from the housing together with its Peltier cooler. The MOPA unit was then mounted in an aluminum housing with a commercial diode collimation objective (Melles Griot 06GLC001) fixed directly in front of the laser chip but without additional beam shaping optics inside the housing. The Peltier element is now cooled by water (flux: 1 l/min) and the housing is constantly flooded with a small flux of nitrogen gas. A Faraday isolator is placed right after the collimation objective (40 dB isolation, 5 mm aperture diameter). To compensate for the astigmatism of the laser output beam the collimation objective is adjusted such that the output beam is collimated in a plane orthogonal to the polarization of the light. In the plane defined by the light polarization and the propagation axis (horizontal plane) a focus appears at a distance of about 84 mm behind the edge of the objective housing. With a cylindrical lens (plane convex, 50 mm focal length, 134.6 mm behind the objective edge) the beam is collimated also in the horizontal plane. The resulting beam has an elliptical cross section (ellipticity about 1:4) which is then circularized by means of an anamorphic prism pair (Melles Griot, 06GPU001). A half-wave plate in front of the prism pair rotates the polarization such that the light is transmitted through the prisms at Brewster's angle. With an additional lens ($f=500$ mm) the beam is focused into the first frequency doubler resonator.

By heating the chip to 50 °C the laser is tuned to 972.5 nm—the wavelength necessary for hydrogen spectroscopy. At this temperature the output power measured directly behind the objective drops to 740 mW while keeping the speci-

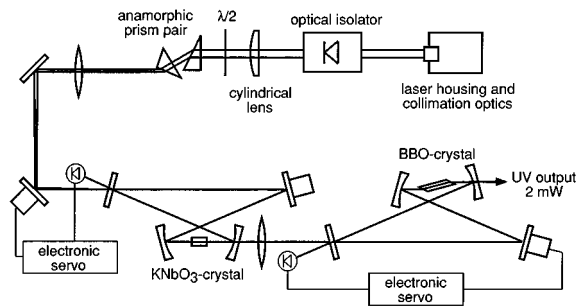


FIG. 1. Experimental setup.

fied operation currents as mentioned above. The power incident on the first doubling cavity is further reduced to 430 mW by the isolator (20% reduction), the lenses (18% reduction), and the prism pair (10% reduction). Neither the lenses nor the prisms are antireflection coated. The reduction due to the isolator is mainly due to the limited aperture which cuts off part of the beam. Figure 2 shows the output power at constant amplifier current but for various master oscillator currents. At certain critical current values the output power exhibits characteristic sharp increases. These increases are accompanied by frequency instabilities which may be observed with the spectrum analyzer. The values of the critical currents depend very strongly on temperature and are reproducible only if the temperature is controlled to better than a tenth of a degree. In addition, a pronounced hysteresis is observed: The solid line in Fig. 2 has been recorded with increasing oscillator current while the dashed line shows the behavior with decreasing current. We assume that these complications are caused by thermal coupling between the power amplifier and the master oscillator.

The first frequency doubler consists of a bow-tie type ring resonator with two identical curved dielectric mirrors (radius of curvature: 25 mm) and two plane dielectric mirrors. A potassium niobate crystal (KNbO_3), (6.5 mm long, b cut for normal incidence, antireflection coated for 972 and 486 nm) is placed halfway between the two curved mirrors. It is mounted with thermal grease to a single quadratic Peltier element (2.25 cm^2) which is cemented onto a water cooled aluminum block with thermally conductive epoxy cement. The temperature of the crystal is electronically controlled with residual temperature fluctuations of less than 10

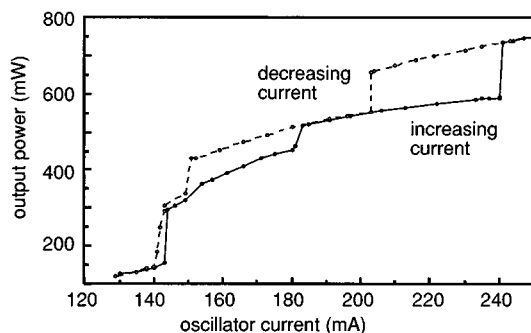


FIG. 2. Output power of the MOPA laser vs injection current of the master oscillator. The amplifier is driven with a current of 3.5 A. The temperature is stabilized to 50 °C.

mK. To tune the resonator, one of the plane mirrors (3 mm thick) is cemented to a high voltage piezoelectric tube (12 mm long, 12 mm diameter, 0.6 mm wall thickness). The other plane mirror (6.2% transmission) serves as an input coupler. Its second surface is uncoated. The separation between the two curved mirrors is 30.7 mm, the incidence angle is 12° , and the total geometrical path length from one of the curved mirrors to the other via the plane mirrors is 196 mm. This geometry produces a circular focused Gaussian beam inside the crystal (waist $w_o = 25 \mu\text{m}$, confocal parameter $b = 4 \text{ mm}$) and a second Gaussian beam with a focus between the two plane mirrors. Its cross section is slightly elliptical (sagittal plane: $w_o = 198 \mu\text{m}$, confocal parameter $b = 251 \text{ mm}$; tangential plane: $w_o = 154 \mu\text{m}$, confocal parameter $b = 154 \text{ mm}$). The input beam is matched to this second waist. The blue light leaves the resonator through one of the curved mirrors (83% transmission at 486 nm). The resonator is covered with a Lucite hood and flooded with nitrogen gas. A biconvex lens ($f = 38.1 \text{ mm}$, uncoated) 29 mm behind the edge of the curved mirror collects the blue light and couples the beam into the second doubler cavity.

As mentioned above, the MOPA laser is very sensitive to feedback from external optical elements. Even by using two successive Faraday isolators (70 dB total isolation) the laser is not decoupled sufficiently but tends to lock to certain frequencies due to parasitic optical feedback. After eliminating all other feedback sources, unavoidable feedback from the antireflection coated input surface of the first Faraday isolator still disturbs the laser. We, therefore, lock the laser to feedback from the frequency doubler cavity¹⁴ which dominates all other feedback sources. One optical isolator (40 dB isolation) suffices to adjust the feedback level. An electronic servo loop controls the phase of the light which is coupled back into the MOPA by means of a mirror that is mounted on a piezo tube. The error signal is generated by a radio frequency modulation technique.¹⁵

At a wavelength near 972.5 nm noncritical type 1 phase matching in KNbO_3 occurs at a temperature of about -16°C . For input powers above 70 mW the losses due to frequency conversion become larger than the passive losses of the resonator, resulting in a linear dependence of the blue output power on the infrared input power. On resonance and with the crystal tuned to optimum second harmonic generation, 30% of the 430 mW infrared input power is reflected at the coated surface of the input coupler. The circulating fundamental power of 3.7 W in the absence of phase matching is reduced by a factor 2.5 when the second harmonic generation is optimized by proper phase matching. The maximum blue output power with the resonator locked on resonance is 156 mW as measured with a pyroelectric power meter directly after the curved cavity mirror. This is, to our knowledge, the highest continuous wave blue output power that has been generated with a semiconductor laser. The measured power is consistent with passive round trip losses of 4.8% and a conversion coefficient of 1.4%/W. The light is emitted in a pure defraction limited Gaussian TEM_{00} mode with a confocal parameter of 1.8 mm. The frequency bandwidth of the emitted light was estimated to be less than 6

MHz by observing the spectrum of the subsequent second doubler stage.

The blue light is coupled into the second doubler stage where a β -barium borate crystal is placed inside a ring resonator similar to the first doubler cavity. The crystal (14 mm long) is cut for Brewster's angle and fixed on a tiltable mount. The two curved mirrors have a radius of 50 mm, the geometrical length of the optical path between the two mirrors is 66.5 mm, and the length of the collimated branch of the resonator via the two plane mirrors is 300 mm. This resonator geometry generates an elliptical beam cross section that is close to the optimum for second harmonic generation.¹⁶ The waist radius in the tangential plane is 39 μm (confocal parameter $b=19$ mm) and in the sagittal plane 22 μm (confocal parameter $b=6$ mm). The focus of the collimated cavity branch has a waist of 107 μm ($b=148$ mm) in the tangential plane and 86 μm ($b=95$ mm) in the sagittal plane. The flat input coupler transmits 1.8% at 486 nm. The resonator may be tuned with the second flat mirror which is mounted on a piezo tube. The resonator is locked on resonance with an electronic servo loop. The error signal is generated by analyzing the polarization of the light that is reflected at the input coupler.¹⁷ On resonance 87% of the incident light is coupled into the cavity. With 156 mW incident light power the circulating power inside the cavity amounts to 6.5 W. The doubling crystal (uniaxial) may be phase matched (type 1) by tilting it around an axis perpendicular to the plane defined by the polarization and the wave vector of the blue light. No temperature stabilization is necessary. The ultraviolet output power is 2.1 mW as measured with a pyroelectric power meter directly behind the curved output coupler. Taking into account the transmission of the output coupler (86%) and the reflection at the surface of the crystal (23%), about 3.17 mW of ultraviolet light are generated inside the crystal. The resulting conversion coefficient of $7.5 \times 10^{-5}/\text{W}$ must be compared to the theoretical value of $1.3 \times 10^{-4}/\text{W}$ which holds for an optimized circular Gaussian beam. The deviation by a factor of about 2 is probably due to the noncircular beam cross section inside the crystal. The ultraviolet output beam has an elliptical cross section due to the walk off effect inside the crystal. However, with cylindrical optics the beam may be circularized and coupled into a nonconfocal optical standing wave resonator. On resonance 20% of the incident power is reflected which implies that at least 80% of the ultraviolet light may be transformed into a defraction limited Gaussian TEM₀₀ mode.

The output frequency may be varied by tuning the first frequency doubler cavity. The tuning range is limited by the optical lock to about 1 GHz at 243 nm. Larger frequency scans of up to 3.2 GHz are possible if the oscillator current is simultaneously varied during the scan. The ultraviolet frequency bandwidth has been estimated with a Fabry-Pérot spectrum analyzer to be smaller than the 20 MHz resolution of the spectrum analyzer. The ultraviolet output power fluctuates less than 3% mainly due to residual acoustic and seis-

mic noise which perturb the resonance frequencies of the doubler cavities. No degradation of the continuous ultraviolet output power has been observed over a period of several hours. This is, up to now, the only solid state continuous wave laser source with a wavelength below 300 nm and an output power level in the range of milliwatts.

It is a particular advantage of our approach that the geometrical properties of the blue and the ultraviolet laser beams are defined primarily by the geometry of the doubler resonators. Even at maximum output power no pointing instabilities or fluctuations of the beam shape or the divergence angle has been observed. This is in contrast to the infrared beam of the MOPA laser which noticeably changes its confocal parameter at high powers such that the mode matching into the first doubler stage has to be optimized for a given laser power.

The ultraviolet frequency doubler has been tested first with a single mode argon ion laser at 488 nm. With 200 mW input power 7.6 mW ultraviolet light has been obtained. However, after cleaning the crystal with a single wipe using acetone and lens cleaning paper, the passive losses of the crystal have increased significantly and the output power has dropped to less than 50%. This indicates that with a new crystal and antireflection coated optics it should be possible to produce more than 200 mW blue light and more than 7 mW ultraviolet radiation with the current setup.

This work has been partially supported by the Deutsche Forschungs Gemeinschaft and by the European Community HCM CT. 930105.

¹D. Welch, *Phys. World* **7**, 35 (1994).

²W. Lenth, W. J. Kozlovsky, and W. P. Risk, *SPIE Proc.* **1499**, 308 (1991).

³M. Haase, J. Qui, J. DePuydt, and H. Cheng, *Appl. Phys. Lett.* **59**, 1272 (1991); H. Jeon, J. Ding, W. Patterson, A. V. Nurmikko, W. Xie, D. Grillo, M. Kobayashi, and R. L. Gunshor, *ibid.* **59**, 3619 (1991).

⁴H. Morkoc, S. Strite, G. B. Gao, M. E. Lin, B. Sverdlov, M. Burns, *et al.*, *J. Appl. Phys.* **76**, 1363 (1994).

⁵G. Hollemann, E. Peik, and H. Walther, *Opt. Lett.* **19**, 192 (1994).

⁶W. J. Kozlovsky, W. P. Risk, W. Lenth, B. G. Kim, G. L. Bona, H. Jaeckel, and D. J. Webb, *Appl. Phys. Lett.* **65**, 525 (1994).

⁷M. M. Fejer, G. A. Magel, D. H. Jundt, and R. L. Byer, *IEEE J. Quantum Electron.* **QE-28**, 2631 (1992); M. Yamada, N. Nada, M. Saitoh, and K. Watanabe, *Appl. Phys. Lett.* **62**, 435 (1993).

⁸C. Zimmermann, R. Kallenbach, and T. W. Hänsch, *Phys. Rev. Lett.* **65**, 571 (1990).

⁹T. Andreae, W. König, R. Wynands, D. Leibfried, F. Schmidt-Kaler, C. Zimmermann, D. Meschede, and T. W. Hänsch, *Phys. Rev. Lett.* **68**, 1923 (1992).

¹⁰M. Weitz, A. Huber, F. Schmidt-Kaler, D. Leibfried, and T. W. Hänsch, *Phys. Rev. Lett.* **72**, 328 (1994).

¹¹R. Kallenbach, C. Zimmermann, D. H. McIntyre, and T. W. Hänsch, *Opt. Commun.* **70**, 56 (1989).

¹²M. Charlton, J. Eades, R. Hughes, D. Horvath, and C. Zimmermann, *Phys. Reports* **24**, 65 (1994).

¹³S. O'Brien *et al.*, *IEEE J. Quantum Electron.* **QE-29**, 2052 (1993).

¹⁴A. Hemmerich, D. H. McIntyre, C. Zimmermann, and T. W. Hänsch, *Opt. Lett.* **15**, 372 (1990); U.S. Patent No. 5,068,546 (26 November 1991).

¹⁵R. W. P. Drever, J. L. Hall, F. V. Kowalski, J. Hough, G. M. Ford, A. J. Munley, and H. Ward, *Appl. Phys. B* **31**, 97 (1983).

¹⁶G. D. Boyd and D. A. Kleinman, *J. Appl. Phys.* **39**, 3597 (1968).

¹⁷T. W. Hänsch and B. Couillaud, *Opt. Commun.* **35**, 441 (1980).